INTERACTION OF TIP LEAKAGE FLOW WITH INCOMING FLOW IN A COMPRESSOR CASCADE EXCEEDING THE STABILITY LIMIT

M. W. Leitner, M. Zippel, S. Staudacher
Institute of Aircraft Propulsion Systems
Stuttgart University
Pfaffenwaldring 6, D-70569 Stuttgart
Germany

Abstract

In axial compressors tip leakage flow is disadvantageous to efficiency and mass flow stability. The interaction of tip leakage flow with incoming flow in a compressor cascade is investigated on a water channel at various tip clearance width and angles of incidence. To study the flow, we considered the movement of inked fluid elements in space and time. By increasing the angle of incidence the flow rate is decreased and the stability limit is exceeded. The arising instability phenomena are described under various conditions. The temporal evolution of a tip leakage vortex breakdown is visualized in detail. A sudden expansion of the vortex with the formation of a recirculation region is observed. This causes a large blockage effect with significant impact on the incoming flow. The stability limit is found. It depends on the tip clearance width. A strong tip leakage vortex supports the beginning of instability.

1. NOMENCLATURE

t	tip clearance	m
C	chord	m
ρ	density	kg/m^3
η	dynamic viscosity	Pa s
v	velocity	m/s
c	absolute velocity	m/s
w	relative velocity	m/s
u	blade speed	m/s
β	flow angle from axial (rotating frame of reference)	°
i	incidence angle	°
Φ	flow coefficient	-
Re	Reynolds number	-

Subscripts

ax	axial direction
1	inlet

2. INTRODUCTION

The flow field in the tip region of an axial compressor is extremely complex. The rotor tip clearance enables the free rotation of the rotor blade row. However, the pressure difference between the pressure and the suction side of compressor rotor blades drives a leakage flow across the tip clearance. An interaction of the tip leakage flow with the boundary layers and the passage flow occurs. In an axial flow compressor, it is well known that a major part of the total loss arises from the blade tip region. The tip clearance is recognized to be disadvantageous to both the efficiency and stability of axial compressors [1]. Previous numerical investigations to the origin of compressor instability indicate that the tip leakage flow has a dominant influence on the stability of the main flow [2–6]. Experimental studies confirm this [7–9]. Simulations illustrate that a tip leakage vortex breakdown occurs inside the rotor at flow rates near the stability limit [3, 4]. The breakdown is characterized by the existence of a recirculation region, which generates a large blockage effect in the tip region of the passage. This may initiate an unstable main flow.

We visualized the interaction of tip leakage flow with incoming flow exemplarily in a water flow channel. All experimental results were obtained in a linear cascade comprising five blades. High blade loading or low flow rates result in an unstable flow. We reduced the flow rate by increasing the incidence and investigated the flow structures and vortex behavior under 2% and 4% of chord tip clearance. These clearances are representative of those that can occur in a multistage compressor [1]. To study the flow, we considered the movement of inked fluid elements in space and time.

3. BACKGROUND

The stable operation of an axial compressor is limited at low mass flows by compressor stall. Stall is associated with a decrease in overall pressure rise and fluctuations of the through-flow. Aerodynamic instability is a great problem of high performance compressor design. Although many researchers have studies on the instability issue for

over 75 years, it is still unable to well predict the stalling behaviors of a new compressor or to contribute much to the design of a more stall resistant machine [10].

For multi-stage, highly loaded compressors the actual position of the stability limit can only be determined at a significant risk in the experiment. Due to the high pressure ratios already the first compressor surge occurrence can cause damage to the system. This results in the need for a difficult advance calculation of the stability limit and on the other hand the early detection of flow instabilities in the operation [2].

In literature two modes of stall inception are described. The long length scale or “modal” stall inception and the short length-scale or “spike” stall inception. Many axial compressors, however, exhibit spike stall inception which is as yet not fully understood [11]. But it is known that local flow separation or the tip leakage flow can be responsible for the spike stall inception. This occurs at high blade loading or low flow coefficients. The flow coefficient Φ is defined as the ratio of the axial component of the flow velocity to the blade speed:

$$\phi = \frac{c_{ax}}{u} \quad (1)$$

When stall occurs, the flow breakdown process nearly always begins in the vicinity of the rotor tips [10]. Recent numerical investigations indicate that the behavior of tip leakage vortex plays a major role in the compressor rotor stall inception [2, 3, 8]. Furukawa et al. [3] investigated the onset of tip leakage vortex breakdown and its growth with a decrease in flow rate. The Navier-Stokes flow simulations reveal a major role of the vortex breakdown in the characteristic of rotor performance (see Fig. 1).

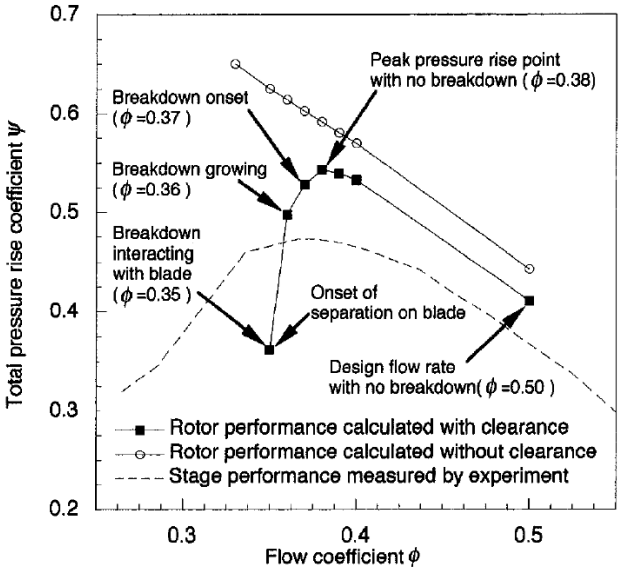

Fig. 1 Total pressure rise characteristic of a rotor [3]

In Fig. 1 square symbols denote results of the Navier-Stokes flow simulations for the rotor with the blade tip clearance. The onset of bubble-type breakdown is observed at Φ = 0.37 where the total pressure rise starts to decrease. As the flow rate is decreased the pressure rise falling further and the breakdown is growing in the streamwise, spanwise, and pitchwise directions.

The associated tip leakage vortex breakdown region in the rotor passage is shown in Fig. 2 [3]. The formation of a recirculation flow zone acts as an aerodynamic blockage. A tip leakage streamline close to the tip leakage vortex center is colored with relative velocity magnitude. The relative velocity along the streamline decreases rapidly in streamwise direction. It is evident that the deceleration of the vortex core flow followed by the recirculation region causes an expansion of the vortex [3]. A bubble-type tip leakage vortex breakdown occurs at the middle of the passage, as also shown in Fig. 3

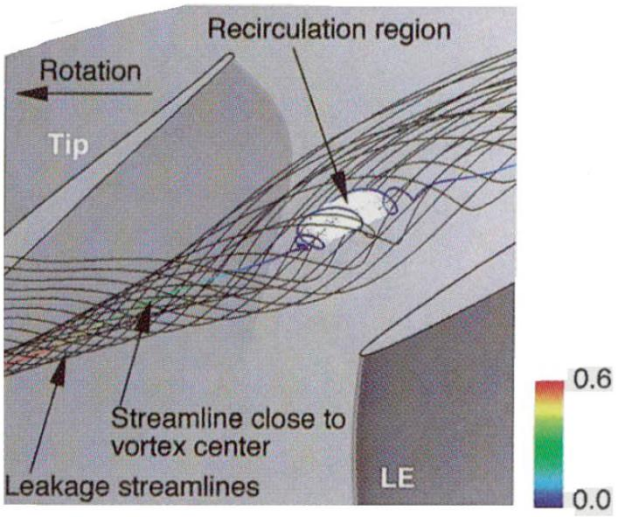

Fig. 2 Streamlines close to tip vortex breakdown region for Φ = 0.37 [3]

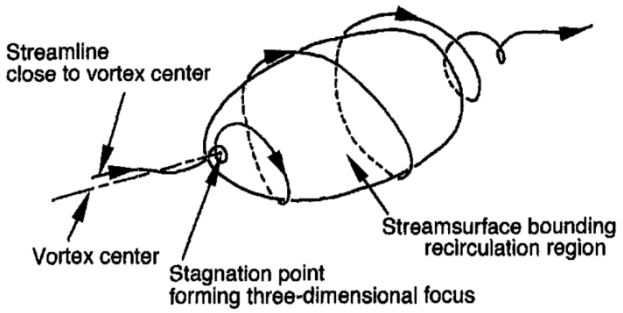

Fig. 3 Flow topology of vortex breakdown [3]

It is known that the distinctive features of vortex breakdown are the occurrence of the large-scale fluctuation in the vortex structure as well as the existence of the stagnation point in the vortex [4]. The onset of breakdown causes significant changes in the nature of the tip leakage vortex. Large expansion of the vortex has an extremely large blockage effect, which has a significant effect on the onset of stall.

In the previous study [12] a comprehensive consideration of the flow structures is carried out in the tip region of the blades. By visualizing the flow a detailed insight in the formation of the tip leakage flow and its interaction is shown. There are two distinguishable flow zones in the blade tip region: the leakage flow region and the incoming flow region (see Fig. 4). A horseshoe vortex appears in the upstream of the incoming flow for every tip clearance. The incoming flow interacts with the tip leakage flow and it rolls up into a vortex. Most of the experiments were done with a fairly high incidence, but the investigations concentrate on stable flow conditions.

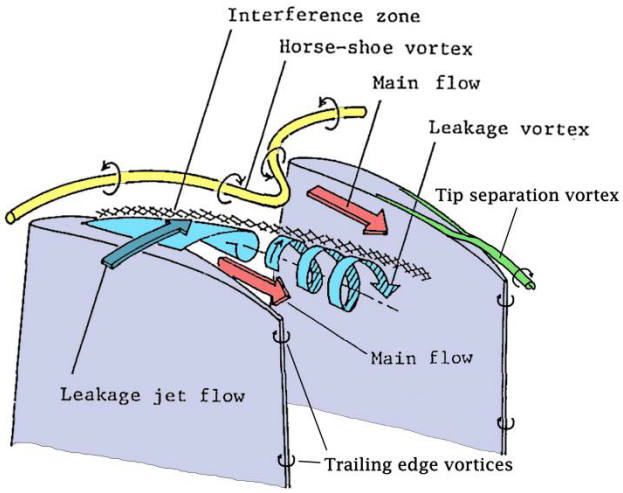

Fig. 4 Flow phenomena at the tip region of the blades [13]

However, for an incidence of 20° or higher, we found unstable flow structures [12]. They differ basically from stable flow structures. A significant blockage of the passage and oscillations were realized. The stability limit is exceeded between 17.5° and 20° incidence. In the present study the stability limit is to be found and the flow phenomena exceeding the stability limit is to be visualized. Criteria for the inception of unstable flow can be found in the compressor cascade.

4. WATER CHANNEL AND EXPERIMENTAL SETUP

All experiments reported in this paper used the water channel at the Institute of Aircraft Propulsion Systems of the University of Stuttgart. A schematic design of the water channel is shown in Fig. 5. Water circulates in a closed circuit. A pump delivers it through a pipe to a reservoir, from where it continues through downpipes to the main basin. This arrangement reduces the influence of the fluctuating pump flow rate. For reducing turbulence, the water passes through a calming section. It consists of a combination of sieves and honeycombs. Afterwards, the water is accelerated through a nozzle and enters the measuring section. After leaving the measurement section, the water enters a collecting basin. The collecting basin leads the water to a water tank, from which the pump is supplied.

A camera installed vertically above the measuring section and a second camera installed horizontally at the side of the measuring section allows the synchronous recording of frames. Hence, the flow phenomena can be simultaneously observed from two orthogonally orientated directions (see e.g. Fig. 9).

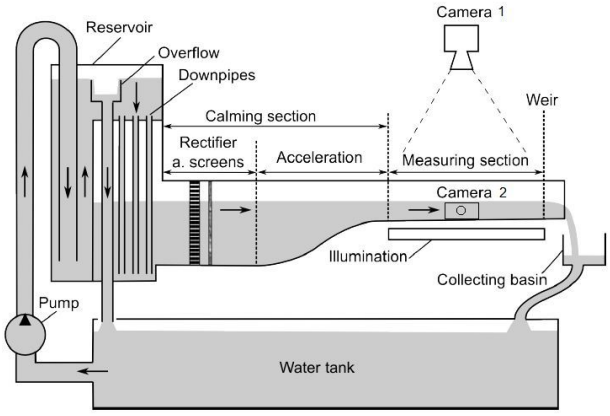

Fig. 5 Schematic design of the water channel [14]

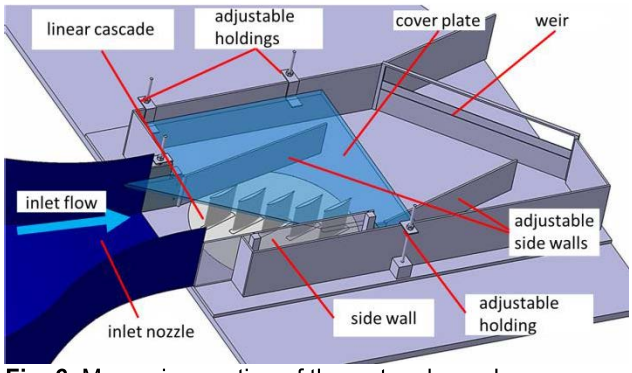

Fig. 6 Measuring section of the water channel

For that purpose, color is added to the flow to observe the flow in its course. Tough pigment is added at the cover plate. Shear forces carry the dye and reveal flow traces of the boundary layer. When inserting dye through probes, the dye has the same density than the surrounding water. The dye is part of the flow and reveals streaklines. These visualization methods are detailed described by Vogt and Zippel (see [15]).

The measuring section is shown in Fig. 6. It comprises the linear cascade with five blades as shown in Fig. 7. The cascade is mounted on a circular plate. We designed the measurement section for a variation of the angle of incidence and the tip clearance. The inlet flow angle of the cascade can be easily altered by turning the circular plate. On water level is a transparent cover plate with vertically adjustable holdings. The height of the cover plate defines the tip clearance.

Flow conditions within the measuring section are set by a weir, in a way which takes care that during a series of measurements the overall mass flow and the water height remain constant. Therefore, for each series of measurements the same average inlet flow velocity into the measuring section is given. On this average inlet flow velocity v an average Reynolds number is established:

(2) $Re = \frac{\rho v C}{\eta}$

The characteristic length, included in the Reynolds number, is the chord length C of the blade. It is also used to create a dimensionless tip clearance. The tip clearance is formulated as per cent of chord.

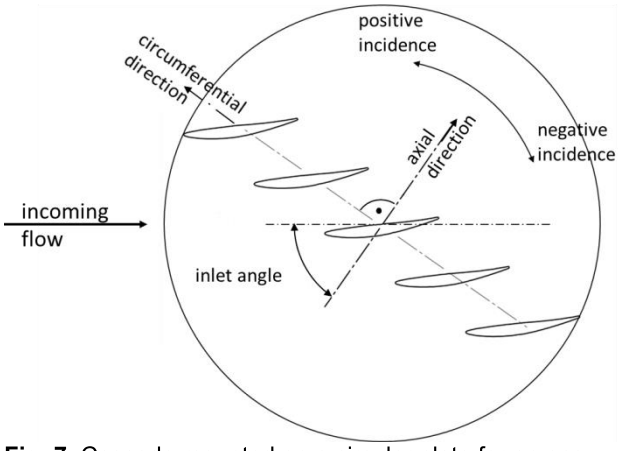

Fig. 7 Cascade mounted on a circular plate for an easy adjustment of the angle of incidence

The periodicity of the flow was controlled by adjustable side walls. This setup is adequate because it is only necessary to achieve the required flow conditions about the central blade. For high incidence angles we additionally used a flap to support the strong deflection of the flow in the side wall region. An ideal inflow of the cascade can be guaranteed even for high incidence.

Because water has a higher viscosity than air, no Reynolds number similarity can be achieved in the water channel. However, it can be assumed that the basic structure of the secondary flow don't change even at considerably higher Reynolds numbers than in the water channel [15].

We used the same NACA-65 blade profile than in the previous study [7]. The NACA-65 is a standard compressor profile. A circular arc is used to define the camber line. The thickness distribution is added symmetrically about the camber line according to Cumpsty [16]. The maximum thickness is 10% of chord. According to Cumpsty the diffusion factor DF = 0.45 is a typical design value [16]. An overview over the cascade design data can be found at Leitner et al. [12].

The linear cascade can be considered as a model of an axial compressor blade row. To regard the rotating frame of reference, we introduce a relative flow angle β and a relative velocity w. We assume the inlet flow is axial. Hence, the absolute inlet rotor velocity is:

(3) $c_1 = c_{\mathrm{ax1}}$

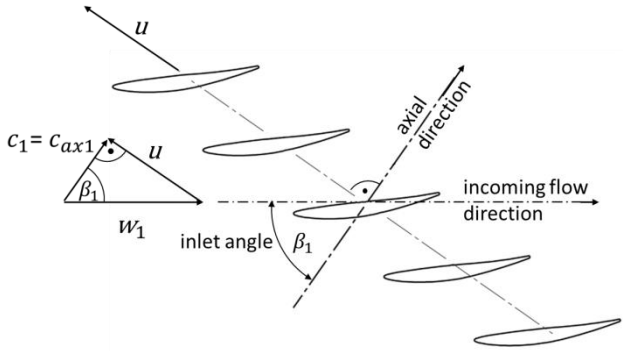

Fig. 8 Velocity triangle of the linear compressor cascade

The relative inlet velocity w_1 can be considered as the inlet velocity of the measuring section. This assumption requires, of course, a matching rotor blade speed u. In Fig. 8 the respective velocity triangle is depicted. The velocity triangle leads to:

(4) $tan\,\beta_1 = \frac{u}{c_{\mathrm{ax1}}}$

With equation (4) we describe the flow coefficient (see equation (1)) as follows:

(5) $\phi_1 = \frac{1}{tan\,\beta_1}$

For design conditions β_1 is the design inlet angle, respectively 55°. To include the off design case, the incidence angle i has to be added:

(6) $\beta_1 = 55° + i$

Finally, we describe the flow coefficient as follows:

(7) $\phi_1 = \frac{1}{tan(55° + i)}$

Hence, the flow coefficient is only a function of the incidence. With the turning of the circular plate the incidence is increased and the flow rate through the cascade is decreased.

5. EXPERMENTAL RESULTS AND DISCUSSION

The essential results are achieved under flow conditions presented in Table 1. We started the measurements at an incidence of 17.5°, where we found a stable flow state in the previous study [12]. Then the incidence is increased

until the stability limit is found. To study the influence of the tip clearance, we distinguish between a small and a large tip clearance at various angles of incidence.

incidence angle i	17.5°	18°	19°
Re≈13000, t/C= 2%	x	x	x
Re≈13000, t/C= 4%	x	x	x

Table 1 Investigated flow conditions

Fig. 9 demonstrate the interaction of the tip leakage flow with the incoming flow for an incidence of 17.5°, 4% of chord tip clearance, and a Reynolds number of 11436. The figure is composed of two parts. The upper part reveals a vertical view and the lower part a horizontal view of the regarded zone. The inlet boundary layer is visualized by green inked fluid elements. The inlet boundary layer first splits because of the high pressure in front of the blades and then enters the passage. The inlet boundary layer moves to the suction side of the adjacent blade. A streakline crossing the tip clearance is visualized by blue inked fluid elements. It can be seen that the inlet boundary layer interacts with the tip leakage flow but don't mix. The area of interaction is highlighted by a red circle in both upper and lower picture. The tip leakage flow rolls up into a vortex and the boundary layer separates from the plate. The phenomena are similar than the phenomena which occur by a lower incidence (see [12]). Fig. 9 shows a stable flow.

Increasing the incidence generates a significant change in the nature of the flow. The tip leakage vortex fluctuates and demonstrates unstable flow phenomena as presented in Fig. 10. In this Figure, it is noticeable that the tip leakage crosses the clearance near mid-chord. However, it doesn't remain there but fluctuates. The pressure difference between the pressure and the suction side of the blade drives the tip leakage across the tip clearance. Hence, a fluctuating tip leakage reveals a fluctuating pressure field in the tip region. Moreover, no fluctuation of the boundary layer is visible. The flow traces and the area of interaction remain always on the same position in spite of fluctuating of tip leakage. The instability doesn't affect the incoming boundary layer.

Further increase of the incidence to 19° (see Fig. 11) increases the frequency of occurrence of unstable phenomena. Also a fluctuating tip leakage flow and an unstable vortex occurs. It seems that a vortex breakdown with a varying nature occurs.

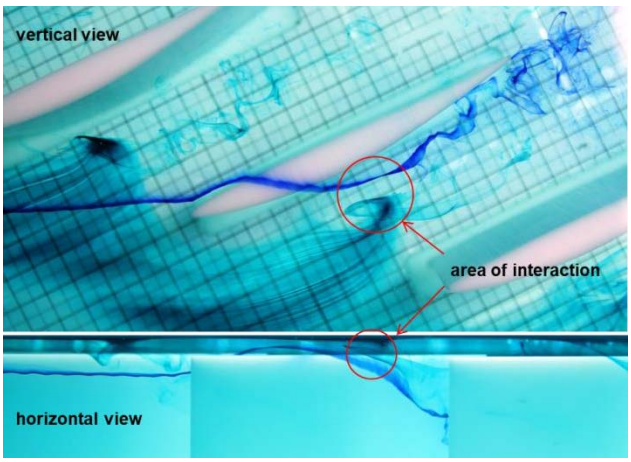

Fig. 9 Interaction of tip leakage flow with incoming flow (i=17.5°, t/C=4%, Re=11436)

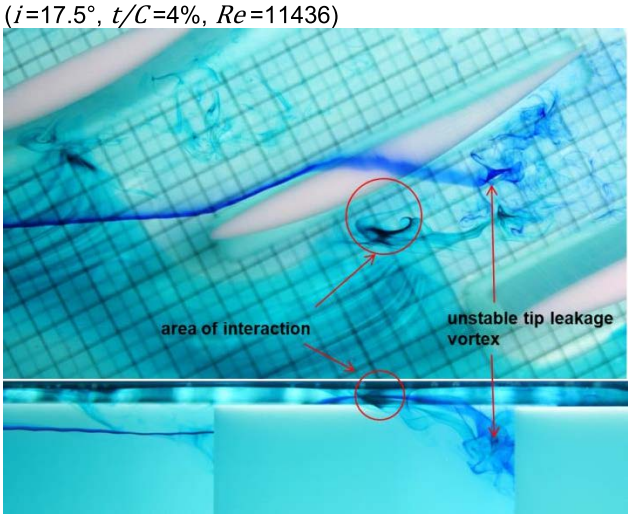

Fig. 10 Interaction of tip leakage flow with incoming flow (i=18°, t/C=4%, Re=11339)

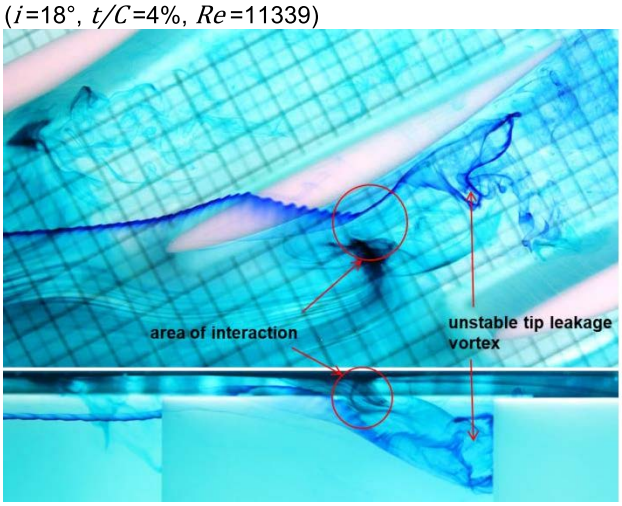

Fig. 11 Interaction of tip leakage flow with incoming flow (i=19°, t/C=4%, Re=11436)

In following figures the interaction of tip leakage flow with incoming passage flow is described. As before, a streakline crossing the tip clearance is visualized by blue inked fluid elements. Instead of the boundary layer a streakline of the passage flow is now visualized by green inked fluid elements. This provides an additional point of view. Fur-

thermore, we may add less dye than before to the flow. Hence, an extend time period can be surveyed without changing the water in the channel.

Fig. 12 and Fig. 13 show the flow at the tip region of the cascade for the same flow conditions. Although the flow conditions are identical, the nature of the flow differs elementarily. For an incidence of 17.5° and a high tip clearance the flow is mainly stable but from time to time unstable flow phenomena occur as shown in Fig. 13. In the stable case the tip leakage flow rolls up into a vortex alongside the suction side of the blade (see Fig. 12). The vortex rotates in clockwise direction. The expansion of the vortex rises downstream until a big part of the tip region of the passage is filled by the vortex. The strong tip leakage vortex results from the large tip clearance and the high incidence. Both strengthen the tip leakage vortex. The tip leakage vortex has a large expansion and therefore, although it is stable, a quit large blockage effect. The tip leakage flow deflects the incoming flow. An obvious deflection of the passage streakline can be observed.

However, there is an occasionally fluctuating of the flow which can result in a blockage of the tip region of the passage. The reason of this blockage is the formation of a tip leakage vortex breakdown. It can be seen in Fig. 13. A bubble-like recirculation region can be observed. It seems to be the same phenomenon as Furukawa et al. [3] has found in their numerical study. In front of this area the flow is decelerated and bended around the recirculation region. To illustrate this region a red ellipse is used in both upper and lower picture. It shall illustrate the roughly dimension of this region but not the exact orientation. In the unstable case the inflow, represented by the green steakline, is deflected much stronger than in the stable case.

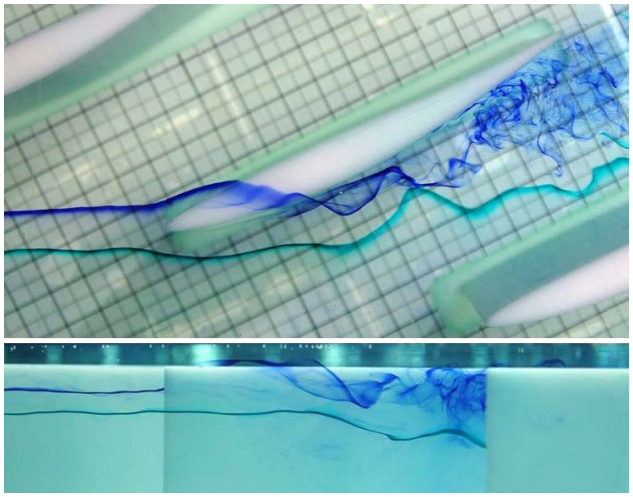

Fig. 12 Stable tip leakage flow (i =17.5°, t/C =4%, Re=13854)

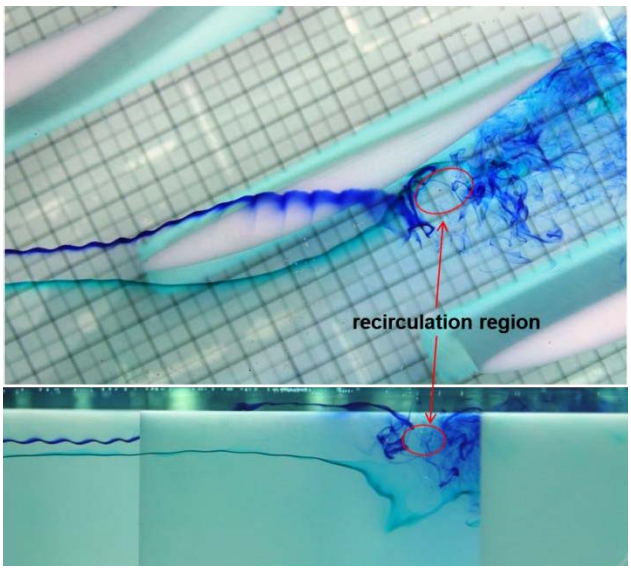

Fig. 13 Unstable tip leakage flow (i =17.5°, t/C =4%, Re=13854)

With increased incidence the instability of the flow increases too. Higher instability induces more intensive fluctuations and an increase of the recirculation region. The increase of the recirculation region with an increase of the incidence Furukawa et al. [3] found too. In Fig. 14 and Fig. 15 a large blockage of the passage, caused by a tip leakage vortex breakdown, is visible. The upper part of Fig. 15 shows clearly how the recirculation region is passed. The unsteady flow nature, caused by the breakdown of the tip leakage vortex in the axial compressor cascade, is visible. The influence of the tip leakage on the stability of the flow becomes obvious. Nevertheless all pictures show only a snap-shot of the flow. The phenomena vary extremely by time. For example, the position where the vortex breakdown takes place may vary from the suction side of the blade to the pressure side of the adjacent blade.

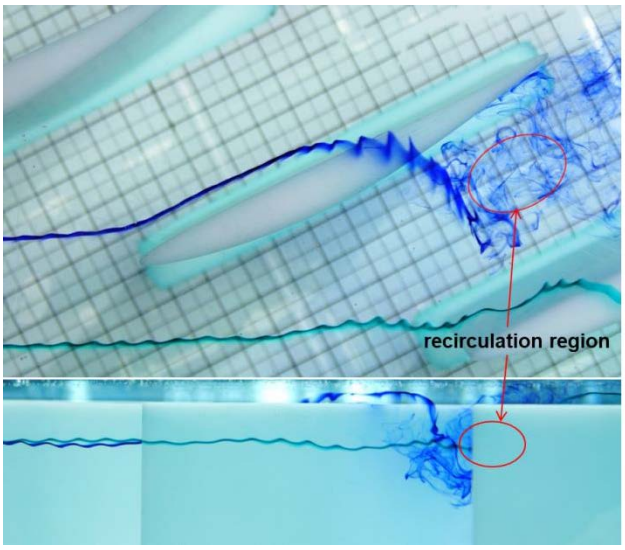

Fig. 14 Unstable tip leakage flow (i =18°, t/C =4%, Re=11749)

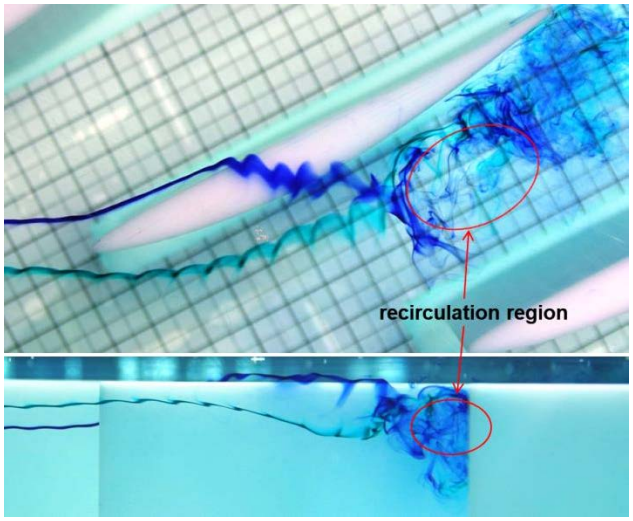

Fig. 15 Unstable tip leakage flow (i =19°, t/C =4%, Re=13854)

Fig. 16, Fig. 17, and Fig. 18 belongs together. They illustrate exemplarily the temporal evolution of a tip leakage vortex breakdown phenomenon. 18 snap-shots were recorded with a frequency of 25 Hz. The top picture of Fig. 16 shows the beginning of this phenomenon, the bottom picture of Fig. 18 shows the end. Accordingly, the tip leakage vortex breakdown phenomenon ends after 680 ms. The vortex breakdown is visualized for an incidence of 19°, a large tip clearance, and a Reynolds number of 13854. A tip leakage streakline close to the vortex center is visualized by blue inked fluid elements. A streakline of the passage flow is visualized by green inked fluid elements.

In the image sequence (see Fig. 16, Fig. 17, and Fig. 18), it can be noticed that the tip leakage flow doesn't move alongside of the suction side of the blade but intrudes into the passage. Then, it moves into the middle of the passage and downstream. After one-third of the duration, a sudden expansion of the vortex is clearly visible (see Fig. 17, red double arrows). This expansion is increasing more and more until almost the entire width of the passage is filled. Consequently, a huge blockage of the passage occurs. After about 480 ms, the maximum vortex expansion is achieved. The green streakline of the passage flow is blocked by the recirculation region of the vortex breakdown. The impact of the recirculation region on the passage flow becomes evident watching the movement of the visualized passage streakline. The arrows A and B mark fluid elements of the streakline (see Fig. 18). The rearward part of the streakline moves faster than the forward part. So, the passages flow has to bypass this obstacle in the middle of the passage. This even affects the tip leakage flow. After the breakdown, the whirling vortex area dissolves and is uniformly transported downstream. This last phase of the phenomena can be described as a turbulent mixing procedure. Du et al. [7] describe it in their experimental study in the same way.

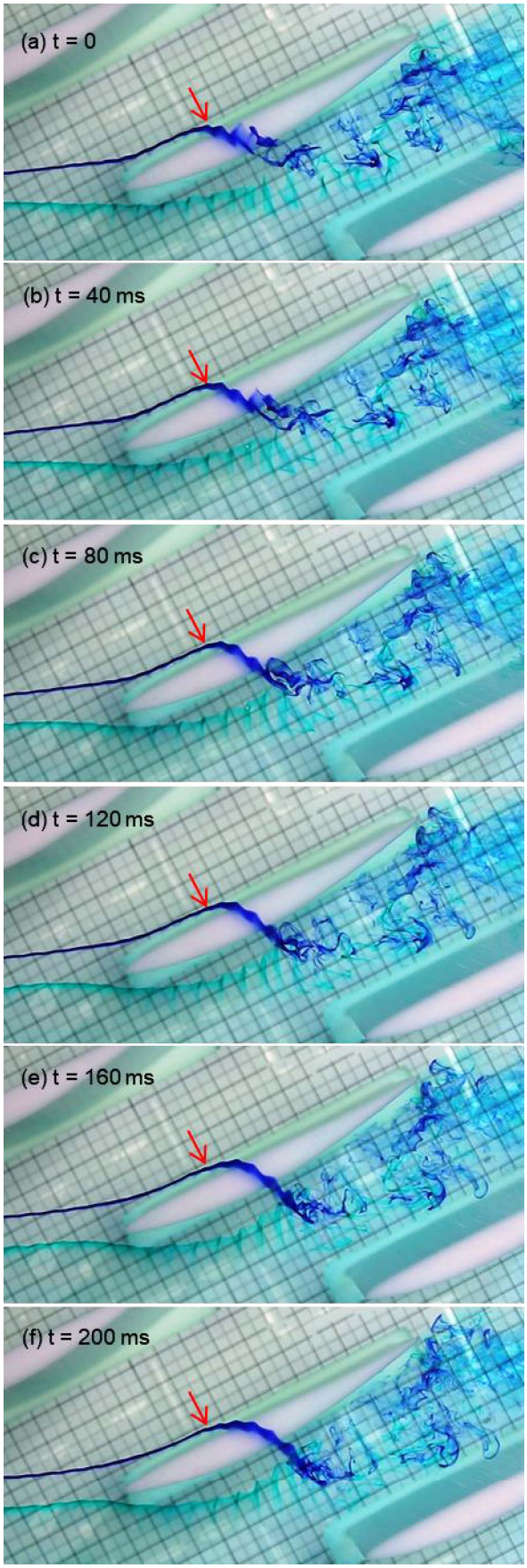

Fig. 16 Temporal evolution of a vortex breakdown - part 1 (i=19°, t/C=4%, Re=13854)

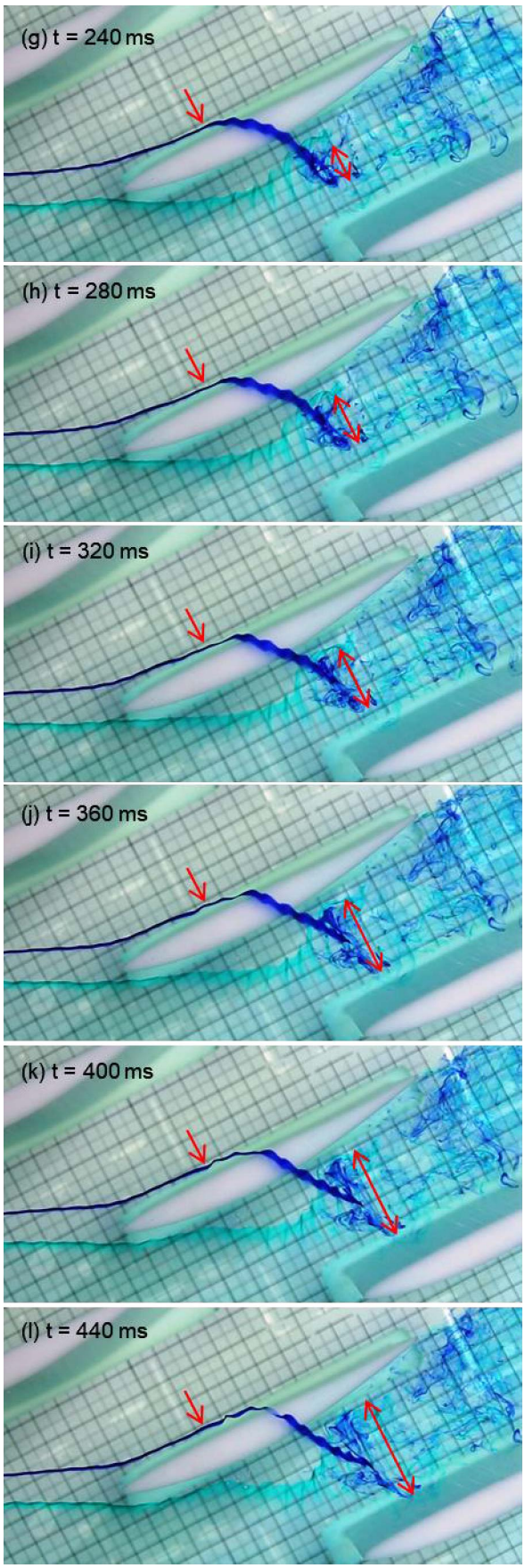

Fig. 17 Temporal evolution of a vortex breakdown - part 2 (i=19°, t/C=4%, Re=13854)

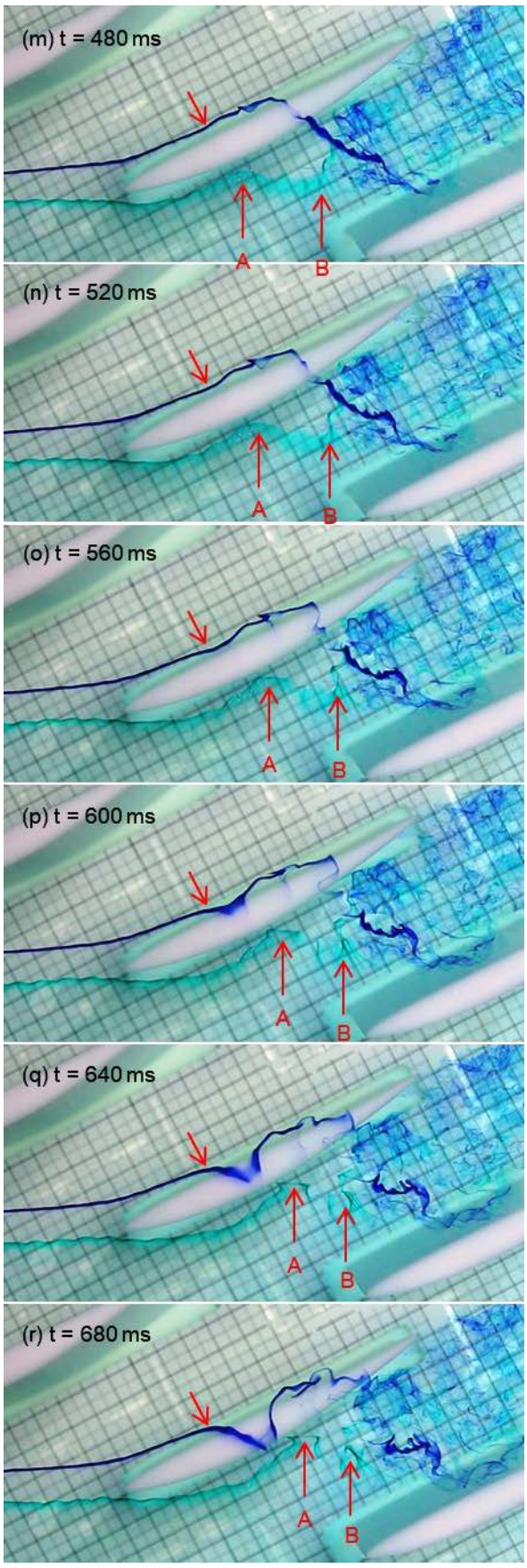

Fig. 18 Temporal evolution of a vortex breakdown - part 3 (i=19°, t/C=4%, Re=13854)

A considerably impact of the vortex breakdown on the tip leakage flow is evident. A blockage of the tip clearance is caused by the tip leakage breakdown and the passage flow passing the obstacle. Temporarily, the tip leakage flow couldn't pass the tip clearance (see Fig. 18) and remains on the suction side of the blade. Hence, the pressure difference between the pressure and the suction side of the blade temporarily dissolves at the tip region. The red arrows in the image sequence at the pressure side of the blade marks the position where the tip leakage flow first enters the tip clearance. After about 640 ms, the tip leakage flow begins to cross the tip clearance again at quit the same position as at the beginning of the phenomenon. After this phenomenon a stable tip leakage vortex may come into being at this position.

There are no regular frequencies in the appearance and disappearance of a tip leakage vortex breakdown phenomenon. However, over time the following process is observed in the unstable flow:

1. Fluctuating, but largely stable tip leakage vortex
2. Sudden expansion of the tip leakage vortex with the formation of a recirculating region
3. The bursting vortex takes largely the entire width of the passage. A blockage effect with significant impact on the incoming flow occurs.
4. Whirling area dissolves and is uniformly transported downstream
5. Formation of a fluctuating but largely stable tip leakage vortex again.

The average duration of this phenomenon is about half a second. A long duration is in coincidence with a large vortex breakdown; a short duration is in coincidence with a small one. A large vortex breakdown may influence also the adjacent passage.

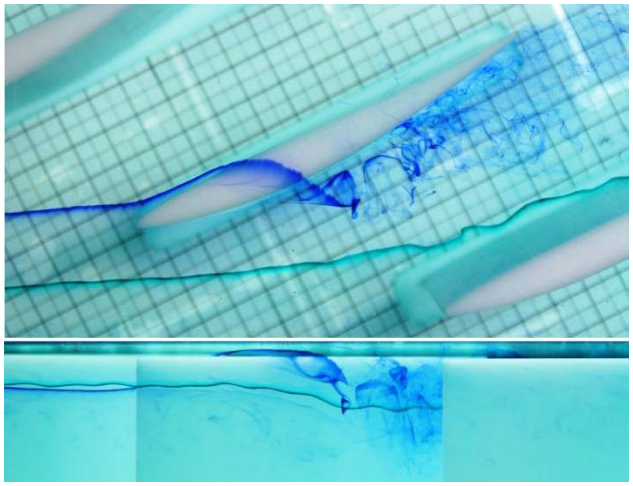

Fig. 19 Stable tip leakage flow (i =18°, t/C =2%, Re=12878)

To study the influence of tip clearance, we also have done measurements with a small tip clearance at various angles of incidence. No noticeable fluctuations and a stable tip leakage vortex are observed by an incidence of 17.5° and 2% of chord tip clearance width. Fig. 19 shows the tip leakage vortex and a passage streakline for an incidence of 18° and 2% of chord tip clearance. Even for this higher incidence no unstable phenomena are visible. The comparison between Fig. 14 and Fig. 19 reveals the influence of tip clearance. Both images present a view of the flow by the same incidence and quite the same Reynolds number, but they differ in tip clearance. A small tip clearance causes a stable flow; a large tip clearance an unstable flow. Hence, a strong tip leakage flow stimulates instability. Increasing the incidence even at a low tip clearance causes instability. Fig. 20 shows a vortex breakdown for a small tip clearance. Even for small tip clearance a considerable blockage effect is visualized.

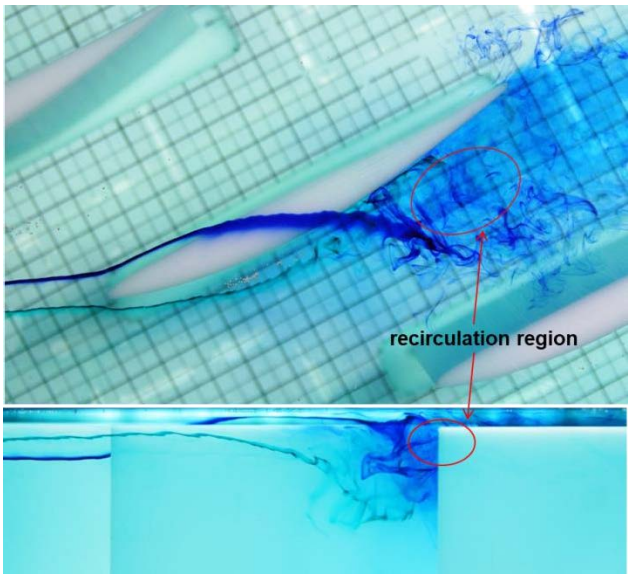

Fig. 20 Unstable tip leakage flow (i =19°, t/C =2%, Re=12878)

In summary, we found that the stable flow state differ significantly from the unstable flow state. The stable tip leakage vortex is located alongside the suction side of the blade; the unstable tip leakage vortex breakdown appears somewhere in the passage. Increased incidence means lower flow rate, increased fluctuations and an increased vortex breakdown rate.

incidence angle i	**17.5°**	**18°**	**19°**
Re≈13000, t/C= 2%	stable	stability limit	unstable
Re≈13000, t/C= 4%	stability limit	unstable	unstable

Table 2 Basic results

Table 2 assembles the basic results due to the stability of the flow. As the stability limit is achieved, small disturbances in the incoming flow can induce instabilities as a vortex breakdown. Further reducing of the flow rate produce the appearance and disappearance of a tip leakage vortex breakdown phenomenon. The rate of this unstable phenomenon is increasing with reducing flow rate. For an incidence of 19° the flow is clearly unstable. The stability limit depends on the tip clearance. A strong tip leakage flow stimulates instability. Hence, the stability limit is found by an incidence of 18° for small tip clearance and by an incidence of 17.5° for large tip clearance. This correlates with a flow coefficient of 0.306 for small tip clearance and a flow coefficient of 0.315 for large tip clearance.

6. CONCLUSIONS

A consideration of the interaction between the tip leakage flow and the incoming flow is carried out. Increasing incidence generates a significant change in the nature of the flow. The tip leakage flow fluctuates and reveals unstable flow phenomena. The unstable flow structure is highly fluctuating with time. Increased incidence means lower flow rate, increased fluctuations and increased vortex breakdown rate.

The temporal evolution process of a vortex breakdown reveals the development of a recirculation region. A temporary blockage of the tip region of the passage occurs. The blockage may extend into the tip clearance. After the vortex breakdown the whirling area dissolves and is uniformly transported downstream. Along with the broken tip leakage vortex moves downstream, the tip leakage flow is rolled up, forming a new vortex.

The stability limit is recognized. It depends on the tip clearance width. A dominant tip leakage vortex supports the beginning of instability. Hence, it is obvious that the tip leakage flow plays an important role for the stability of the flow.

A criterion for tip leakage blockage behavior, which is associated with spike stall inception, is found in the water channel. It is the tip leakage vortex breakdown. The water channel results show a significant similarity to the vortex breakdown phenomena found by Furukawa [3]. Details of this phenomenon are only partly known, but it may explain the spike type stall. If a vortex breakdown occurs in a passage, the main flow is forced to go down and sideways. Especially the deflection on adjacent passages and as a consequence the disturbance of the incoming flow may induce stall.

ACKNOWLEDGMENTS

A lot of the work reported here was done by two students. Mirijam Weimer helped to design the measuring section. Stefan Erhard undertook experiments. The authors would like to thank them.

References

[1] Storer, J. A., and Cumpsty, N. A., “Tip Leakage Flow in Axial Compressors,” *ASME Journal of Turbomachinery*, Vol. 113, 1991, pp. 252–259.

[2] Rick, H., *Gasturbinen und Flugantriebe. Grundlagen, Betriebsverhalten und Simulation*, Springer Vieweg, Berlin, Heidelberg, 2013.

[3] Furukawa, M., Inoue, M., Saiki, K., and Yamada, K., “The Role of Tip Leakage Vortex Breakdown in Compressor Rotor Aerodynamics,” *ASME Journal of Turbomachinery*, Vol. 121, 1999, pp. 469–480.

[4] Furukawa, M., Saiki, K., Yamada, K., and Inoue, M., “Unsteady Flow Behavior Due to Breakdown of Tip Leakage Vortex in an Axial Compressor Rotor Near Stall Condition,” *ASME Proceedings*, 2000.

[5] Vo, H., D., *Role of Tip Clearance Flow on Axial Compressor Stability*, 2001.

[6] Hoying, D., A., Tan, C., S., Vo, H., D., and Greitzer, E., M., “Role of Blade Passage Flow Structures in Axial Compressor Rotating Stall Inception,” *ASME Proceedings*, 1998, pp. 98-GT-588.

[7] Du, H., Yu, X., Zhang, Z., and Liu B., “Relationship between the Flow Blockage of Tip Leakage Vortex and its Evolutionary Procedures inside the Rotor Passage of a Subsonic Axial Compressor,” *Journal of Thermal Science*, Vol.22, No.6, 2013.

[8] Hewkin-Smith, M., Pullan, G., Grimshaw, S. D., Greitzer, E., M., and Spakovszky, Z. S., “The Role of Tip Leakage Flow in Spike-Type Rotating Stall Inception,” *ASME Proceedings*, 2017.

[9] Zhang, Z., Yu, X., and Liu B., “Characteristics of Tip Leakage Vortex in a Low-Speed Compressor with different Rotor Tip Gaps,” *ASME Proceedings*, GT2012-69148, 2012.

[10] Day, I. J., “Stall, Surge, and 75 Years of Research,” *ASME Journal of Turbomachinery*, 2016.

[11] Tan, C., S., Day, I., Morris, S., and Wadia, A., “Spike-Type Compressor Stall Inception, Detection and Control,” *Annual Review of Fluid Mechanics*, Vol. 42, 2010, pp. 275–300.

[12] Leitner, M. W., Zippel M., and Staudacher S., “The Interaction of Tip Leakage Flow with Incoming Flow in a Compressor Cascade,” *DLR Kongress*, Vol. 420023, 2016.

[13] Inoue, M., and Kuroumaru, M., “Structure of Tip Clearance Flow in an Isolated Axial Compressor Rotor,” *ASME Journal of Turbomachinery*, Vol 111, 1989, pp. 250–256.

[14] Georgi J., Staudacher S., “Characteristics of Ejectors on Small Gas Turbine Engines,” *DLR Kongress*, Vol. 301339, 2013.

[15] Vogt, H., and Zippel M., “Sekundärströmungen in Turbinengittern mit geraden und gekrümmten Schaufeln; Visualisierung im ebenen Wasserkanal,” *Forschung im Ingenieurwesen*, Vol. 62, 1996, pp. 247–253.

[16] Cumpsty, N. A., *Compressor Aerodynamics*, Krieger Publishing Company, Malabar, Florida, 2004.